

Comparative Study of Structural, Electronic, Magnetic and Thermodynamic Properties of TbInZ_2 ($Z = \text{Cu, Ag, and Au}$)

A. TOUIA^{a,*}, K. BENYAHIA^a,
I.S. MESSAOUDI^a AND A. TEKIN^b

^aMaterials Science and Applications Laboratory, Faculty of Sciences and Technology, University of Ain Temouchent, Belhadj Bouchaib. BP 284, Ain-Temouchent, 46000, Algeria

^bInformatics Institute, Istanbul Technical University, 34469 Maslak, Istanbul, Turkey

Received: 18.11.2021 & Accepted: 03.01.2022

Doi: [10.12693/APhysPolA.141.210](https://doi.org/10.12693/APhysPolA.141.210)

*e-mail: dr.a.touia2020@gmail.com

Structural, electronic, magnetic and thermodynamic properties of TbInZ_2 ($Z = \text{Cu, Ag, and Au}$) materials with two types of Heusler regular and inverse structures have been investigated in the framework of density functional theory. The non-magnetic, ferromagnetic and antiferromagnetic states are presented using first principles calculations. We applied the full potential linearized augmented plane waves method implemented in the Wien2k code, and the generalized gradient approximation was used to describe the exchange–correlation potential. The results obtained for the density of states and band structures reveal the metallic character of the studied compounds. The structural properties show that the most stable state for TbInZ_2 ($Z = \text{Cu, Ag, and Au}$) compounds is the ferromagnetic state. The magnetic susceptibility and electrical Conductivity as a function of chemical potential are calculated using Perdew–Burke–Ernzerhof generalized gradient approximation. Furthermore, the variations of the lattice parameter, heat capacity, Debye temperature and entropy as a function of temperature have been investigated.

topics: magnetic susceptibility, electrical conductivity, Wien2k, Debye temperature

1. Introduction

TbInZ_2 ($Z = \text{Cu, Ag, Au}$) materials have a variety of properties which are very interested in many fields such as spintronics [1]. In order to describe these different characteristics, simulation is necessary to predict the various properties of such innovative materials since fascinating phenomena in rare earth containing materials arise from the complex interaction between local rare earth “4*f*” electrons and roaming “*s, p, d*” electrons. The TbInZ_2 ($Z = \text{Cu, Ag, Au}$) materials were synthesized with a composition alike to full-Heusler L2_1 (group no. 225) [2–4]. In fact, the structure was clarified from X-ray powder diffraction using Cr $K_{\alpha 1}$ and Cr $K_{\alpha 2}$ radiation [2–4] and the TbInZ_2 ($Z = \text{Cu, Ag, Au}$) alloys are ferromagnetically ordered at $T = 0$ K and $P = 0$ Gpa. Recently, the full-Heusler are divided into two types of structures:

- the regular Heusler L2_1 which corresponds to the space group $Fm\bar{3}m$ (no. 225), where the elements Z_1 , Z_2 , Y, and X, respectively, occupy the positions (0, 0, 0) (1/2, 1/2, 1/2), (1/4, 1/4, 1/4) and (3/4, 3/4, 3/4) [5];

- the second structure is the inverse Heusler C1_b in the cubic $F\bar{4}3m$ space group (no. 216), the occupied positions are Z_1 (0, 0, 0), Z_2 (1/4, 1/4, 1/4), Y (1/2, 1/2, 1/2) and X (3/4, 3/4, 3/4), respectively, (see Fig. 1) [5].

In this work, we performed calculations according to first principles using the full potential linearized augmented plane waves (FP-LAPW) [6–8] method

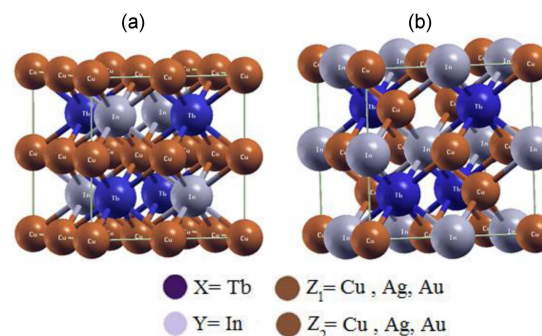


Fig. 1. (a) Regular and (b) inverse structure for XYZ_2 ($Z = \text{Cu, Ag, Au}$) Heusler compounds.

TABLE I

Lattice constant a_0 [Å], bulk modulus B [GPa], and its pressure derivative B' using GGA-PBE for three states, non-magnetic (NM), ferromagnetic (FM) and antiferromagnetic (AFM).

Structures	States	a_0 [Å]	B_0 [GPa]	B'
TbInCu ₂				
regular structure	NM	6.6894	74.6	4.8
	FM	6.6769	85	4.1
	AFM	6.6773	81.3	4.6
inverse structure	NM	6.7529	68	4.7
	FM	6.7441	76.2	4.2
	AFM	6.7470	71.4	4.8
exper. [1]		6.616	–	–
TbInAg ₂				
regular structure	NM	7.1018	66.3	3.7
	FM	7.0507	67.7	4.8
	AFM	7.0504	65	5.1
inverse structure	NM	7.0933	58.9	4.7
	FM	7.0672	63.3	4.8
	AFM	7.0680	60.7	5
exper. [2]		6.934	–	–
TbInAu ₂				
regular structure	NM	7.0551	74.1	5.1
	FM	7.0359	77.2	5.8
	AFM	7.0432	76.2	5.2
inverse structure	NM	7.0349	80.4	3.8
	FM	7.0087	82	5.1
	AFM	7.0048	77.5	5.4
exper. [3]		6.913	–	–

based on the density functional theory and implemented in the Wien2k code [7, 8]. The generalized gradient approximation [7–10] was used to describe the exchange-correlation potential.

2. Computational method

We have used full-potential linearized augmented plane wave (FP-LAPW) [6–9] method based on density functional theory and implemented in the Wien2K code [8, 9]. Indeed, in our calculations of TbInZ₂ (Z = Cu, Ag, and Au) materials with two types of Heusler regular and inverse structures, a generalized gradient approximation GGA-PBE [8–11] was applied in three states: non-magnetic (NM), ferromagnetic (FM) and antiferromagnetic (AFM). The wave functions, electron densities and potential are developed on the basis of spherical harmonic combination multiplied by the radial functions within the non-overlapped spheres that surround the atomic sites (muffin-tin sphere). That is to say, the quantum orbital number (cut-off radius) was limited to $l_{\max} = 10$ on a plane wave with a cut-off radius $Rk_{\max} = 8$ basis in

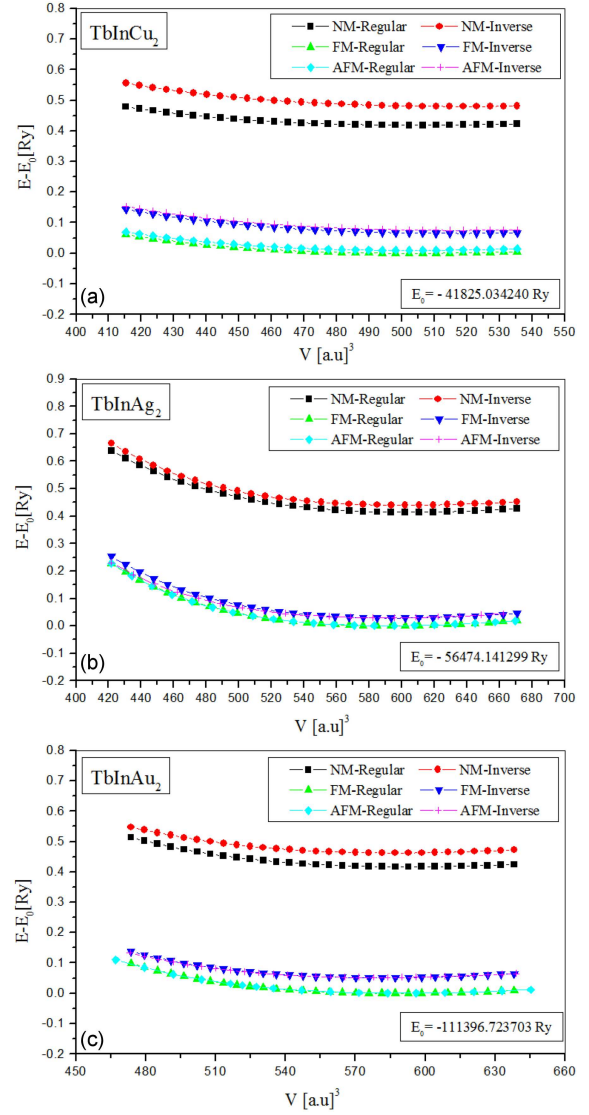


Fig. 2. (a, b, c) Normalized energy as a function of volume of TbInZ₂ (Z = Cu, Ag, Au) using GGA-PBE approximation for the three states, non-magnetic (NM), ferromagnetic (FM) and antiferromagnetic (AFM), at regular and inverse structure Heusler.

the rest of space (interstitial region), where R_{mt} is the smallest radius of the muffin-tin sphere. The value of muffin-tin radii of Tb, In, Z = Cu, Ag, Au atoms is 2.5 Bohr, where k_{\max} is the modulus of the largest vector of the reciprocal lattice. The Fourier development of the charge density was performed for the wave vector $G_{\max} = 12$. For the integration of the first Brillouin zone, 47k points are used for the three compounds. Thus, the convergence of each self-consistent calculation is necessary to optimize the structural properties, and the iteration is repeated until the total energy converges to less than 10^{-4} Ry. The energy separating the valence states and those of the heart is $E_{\text{cut}} = -6$ Ry.

3. Results and discussion

3.1. Structural properties

The exchange and correlation potential has been treated in this work by the approximation of the generalized gradient GGA-PBE [8–11] for two types of Heusler structures (regular and inverse) [12]. The stabilization of the non-magnetic or magnetic state (ferromagnetic or antiferromagnetic) is determined from the minimization of energy as a function of volume using the Murnaghan equation of state (EOS) [13]. The optimization curves of the total energies of TbInZ_2 ($Z = \text{Cu, Ag, Au}$) alloys in three states non-magnetic, ferromagnetic and antiferromagnetic for two types of Heusler structures (regular and inverse) are shown in Fig. 2. It is clear that the most stable structure for the TbInZ_2 ($Z = \text{Cu, Ag, Au}$) compounds corresponds well to the type of regular Heusler structures, and the results are leading to a more stable ferromagnetic configuration in comparison to non-magnetic and antiferromagnetic configurations for all three compounds. The calculated values of the crystal parameters and the bulk modulus B_0 for the TbInZ_2 ($Z = \text{Cu, Ag, Au}$) alloys are summarized in Table I and compared with some experimental results from the literature [2–4]. A good agreement is found.

3.2. Electronic and magnetic properties

The band structures of TbInZ_2 ($Z = \text{Cu, Ag, Au}$) compounds were calculated using the values of the theoretical lattice parameters, which we obtained by the FP-LAPW method based on density functional theory (DFT) and implemented in the Wien2K code. Figures 3–5 show the band structures obtained by GGA-PBE for the compounds TbInZ_2 ($Z = \text{Cu, Ag, Au}$) in the spin majority and minority directions according to the directions of the high symmetry in the Brillouin zone [14]. For the majority and minority spin configurations considered, the gap values are zero. These compounds are

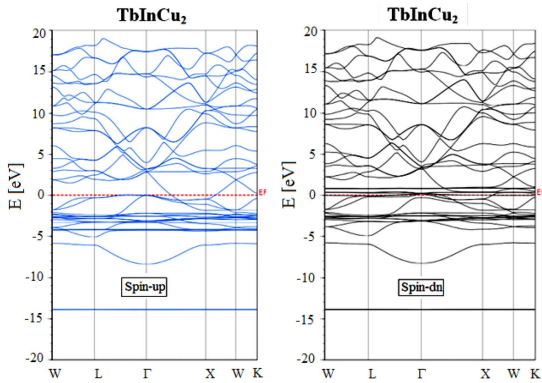


Fig. 3. The band structure of TbInCu_2 in ferromagnetic (FM) state using GGA-PBE approximation with spin polarization at regular structure Heusler.

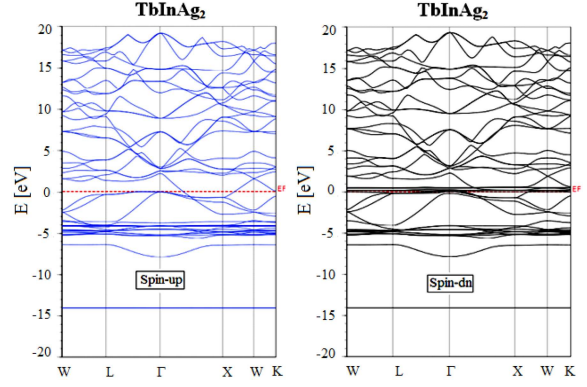


Fig. 4. The band structure of TbInAg_2 in ferromagnetic (FM) state using GGA-PBE approximation with spin polarization at regular structure Heusler.

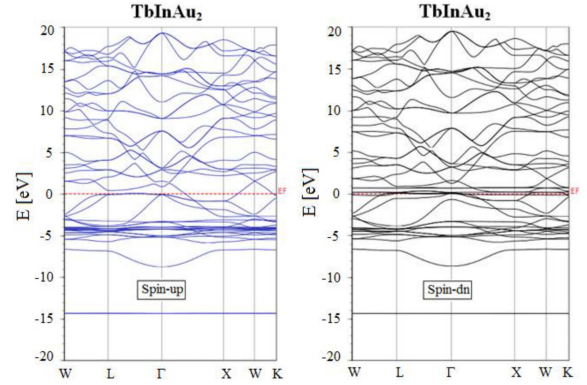


Fig. 5. The band structure of TbInAu_2 in ferromagnetic (FM) state using GGA-PBE approximation with spin polarization at regular structure Heusler.

therefore ferromagnetic metals. Indeed, we notice the non-homogeneity of the band structures of TbInZ_2 ($Z = \text{Cu, Ag, Au}$) alloys in the direction of majority and minority spin, which indicates that the spin polarization at the Fermi level is not zero.

Electronic charge density is also another way to study the electronic properties of these compounds. Figures 6–8 give the predicted results of the total and partial density of states [15] of TbInZ_2 ($Z = \text{Cu, Ag, Au}$) alloys calculated by the GGA-PBE. We notice the predominant f state of the Tb atom at the Fermi level and the valence band. However, a small contribution of the d state of Cu, Ag and Au atoms is present at higher levels of the valence band. The lowest level of the valence band is clearly occupied by the d state of the In atom for the two compounds TbInCu_2 and TbInAu_2 . The total and local spin magnetic moment of each element per unit cell of TbInZ_2 ($Z = \text{Cu, Ag, Au}$) materials are calculated using the generalized gradient approximation GGA-PBE to understand the magnetic interactions. The results are listed in Table II.

TABLE II

Total and local magnetic moment of TbInZ_2 ($Z = \text{Cu, Ag, Au}$) at $T = 0 \text{ K}$ and $P = 0 \text{ GPa}$ obtained using GGA-PBE approximation with spin polarization (in ferromagnetic state).

	Magnetic moment [μ_B]				
	Tb	In	Z = Cu, Ag, Au	Interstitial	Total
TbInCu_2	5.91535	-0.01121	0.00865 (Cu)	0.08458	6.00603
TbInAg_2	5.82209	-0.01957	-0.00515 (Ag)	0.11366	5.90588
TbInAu_2	5.82029	-0.00724	0.00024 (Au)	0.09164	5.90518

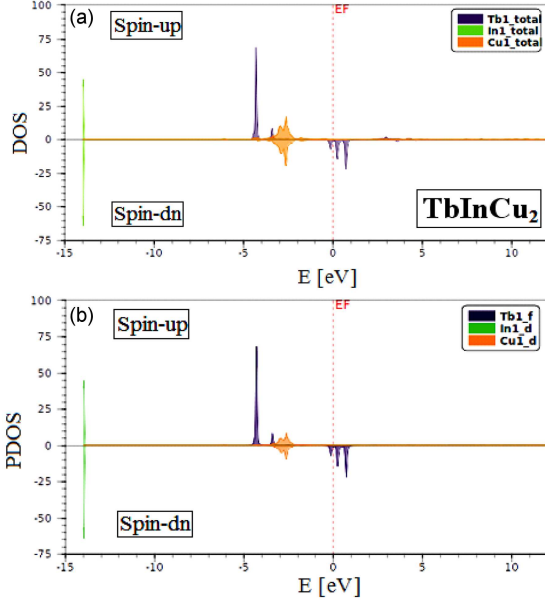


Fig. 6. The total and partial density of states of TbInCu_2 in ferromagnetic (FM) state using GGA-PBE approximation with spin polarization at regular structure Heusler.

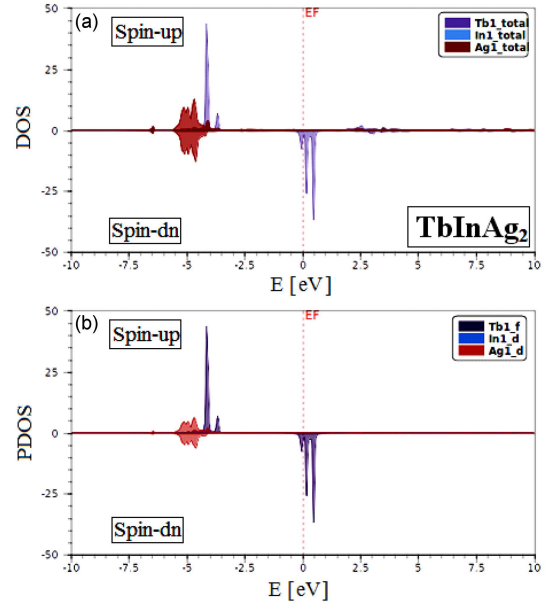


Fig. 7. The total and partial density of states of TbInAg_2 in ferromagnetic (FM) state using GGA-PBE approximation with spin polarization at regular structure Heusler.

The value of the total magnetic moment in the three alloys comes mainly from the Tb atom and the low contribution of Cu, Ag and Au atoms. On the other hand, the contribution of In atom is almost negligible. These results are likely to give rise to a ferromagnetic character between the electrons of the f state of the Tb atom and the electrons of the d state of the In, Cu, Ag and Au atoms.

The magnetic susceptibility (χ) and electrical conductivity of the compounds are computed by employing the BoltzTrap code [22]. The variation of the magnetic susceptibility (χ) [16] as a function of the chemical potential is shown in Fig. 9. It is clearly seen that the highest values of the magnetic susceptibility are found in the two compounds TbInAg_2 and TbInAu_2 . The curves show a maximum value of the magnetic susceptibility of $\approx 3.43 \times 10^{-8} \text{ m}^3/\text{mol}$ corresponding to the chemical potential value of 0.542 eV and $3.09 \times 10^{-8} \text{ m}^3/\text{mol}$ corresponding to the chemical potential value of 0.562 eV for the two compounds TbInAg_2 and TbInAu_2 , respectively. For the material TbInCu_2 , the magnetic susceptibility is higher compared to the other two materials

TbInAg_2 and TbInAu_2 in the interval from 0.39 eV to 0.49 eV of the chemical potential and then at 0.492 eV of the chemical potential. The value of the magnetic susceptibility gradually decreases until reaching zero for the material TbInCu_2 . When the magnetic susceptibility is weakly positive, the TbInZ_2 ($Z = \text{Cu, Ag, Au}$) materials have a paramagnetic character. These materials become paramagnetic beyond the Curie temperature.

The variation of electrical conductivity [9, 17] as a function of chemical potential is displayed in Fig. 10. Our results show that the maximum electrical conductivities at $1.14 \times 10^{21} (\Omega \text{ cm s})^{-1}$, $1.03 \times 10^{21} (\Omega \text{ cm s})^{-1}$ and $9.62 \times 10^{20} (\Omega \text{ cm s})^{-1}$ are obtained for a chemical potential at 0.467 eV, 0.458 eV and 0.437 eV for the three compounds TbInCu_2 , TbInAg_2 and TbInAu_2 , respectively. Therefore, the electrical conductivity is high and thus the current is free to flow. All the three compounds exhibit approximately the same behavior, and the curves show that they have a metallic character. The more electrically conductive a material is, the less resistance it offers to the current flow.

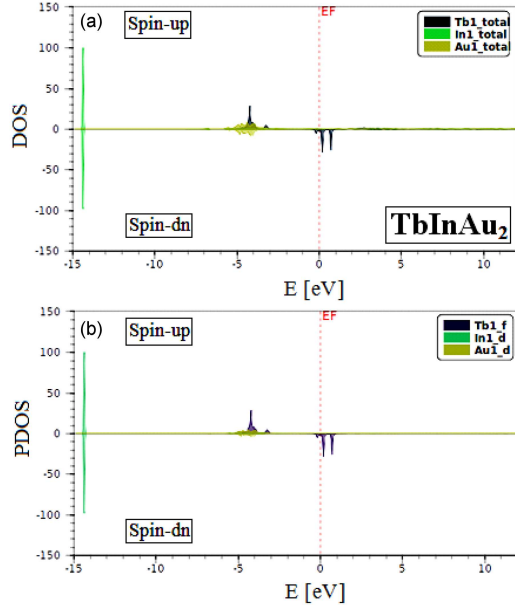


Fig. 8. The total and partial density of states of TbInAu_2 in ferromagnetic (FM) state using GGA-PBE approximation with spin polarization at regular structure Heusler.

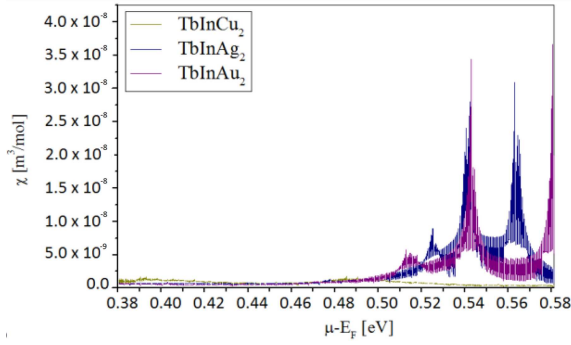


Fig. 9. The magnetic susceptibility (χ) as a function of chemical potential for TbInZ_2 ($Z = \text{Cu, Ag, Au}$) in ferromagnetic (FM) state using GGA-PBE approximation at regular structure Heusler.

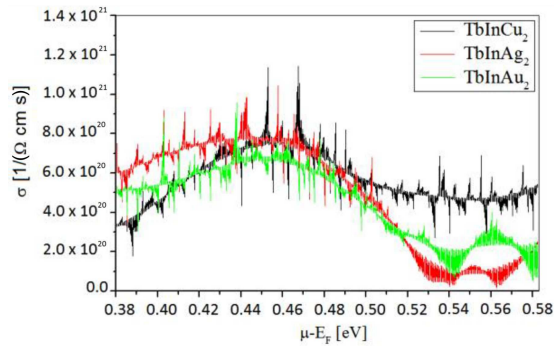


Fig. 10. The electrical conductivity (σ) as a function of chemical potential for TbInZ_2 ($Z = \text{Cu, Ag, Au}$) in ferromagnetic (FM) state using GGA-PBE approximation at regular structure Heusler.

3.3. Thermodynamic properties

The thermal properties are determined in the temperature range from 0 to 800 K for the three compounds TbInZ_2 ($Z = \text{Cu, Ag and Au}$) where the quasi-harmonic model [18] remains fully valid. The pressure effect is studied in the range 0–20 GPa for all three compounds. The effects of temperature on the lattice parameter are represented for three compounds in Fig. 11a–c. Note that for a given pressure value, the lattice parameter increases with the increase of temperature. While, for a determined temperature, the mesh parameter is inversely proportional to pressure.

Figures 12a–c and 13a–c represent the variation of the heat capacity C_V and C_P as a function of temperature for different values of pressure. We notice that at low temperatures, C_V and C_P are proportional to T^3 . However, in high temperatures ($T > 400$ K), C_P always has this increasing rate and C_V tends towards a linear regime.

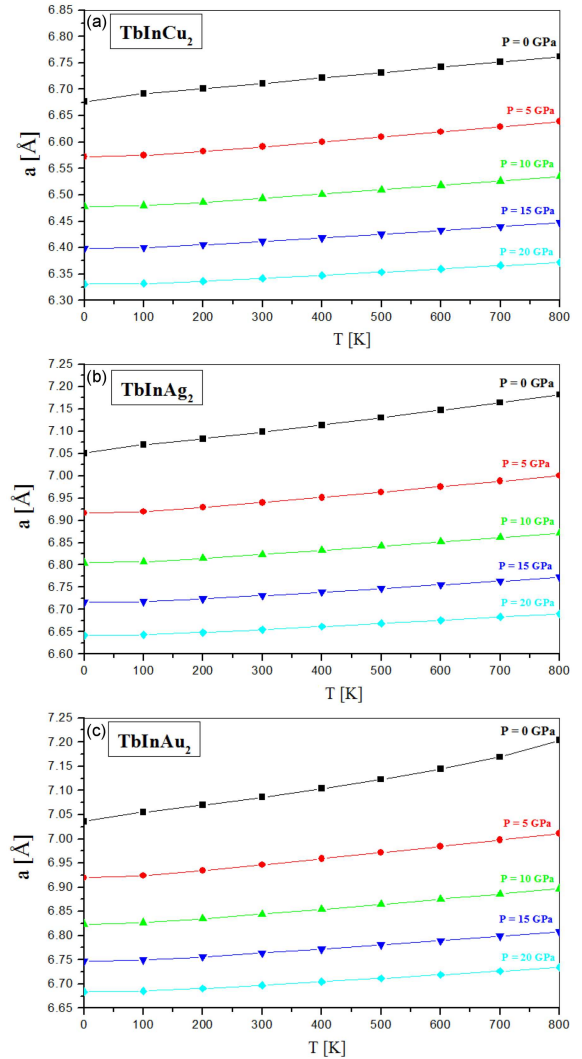


Fig. 11. (a, b, c) The variation of lattice parameter as a function of temperature for TbInZ_2 ($Z = \text{Cu, Ag, Au}$) at different pressures.

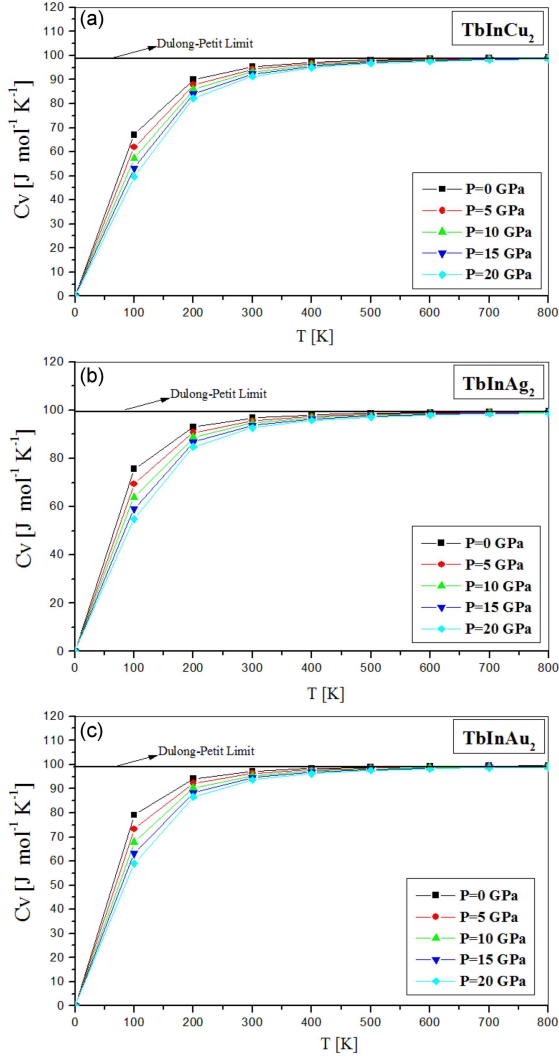


Fig. 12. (a, b, c) The variation of heat capacity C_v as a function of temperature for TbInZ_2 ($Z = \text{Cu}, \text{Ag}, \text{Au}$) at different pressures.

This is the Dulong–Petit limit [19–21], which is equal to 99.02 J/(mol K), 99.94 J/(mol K) and 99.48 J/(mol K) for the compounds TbInCu_2 , TbInAg_2 and TbInAu_2 , respectively.

The results relating to the Debye temperature θ_D are displayed in Fig. 14a–c. We can notice that θ_D is almost constant from 0 to 100 K then decreases linearly with temperature for $T > 200$ K. Whereas, the Debye temperature increases linearly with pressure for a constant temperature. The static values of the Debye temperature (at $T = 0$ K and $P = 0$) calculated from the quasi-harmonic model for three compounds TbInCu_2 , TbInAg_2 and TbInAu_2 are 294.79 K, 244.3 K and 222.49 K, respectively.

The variation of entropy S as a function of temperature at different pressures for the compounds TbInCu_2 , TbInAg_2 and TbInAu_2 is shown in Fig. 15a–c. For a given pressure, entropy S increases sharply with increasing temperature and decreases with increasing pressure at a given

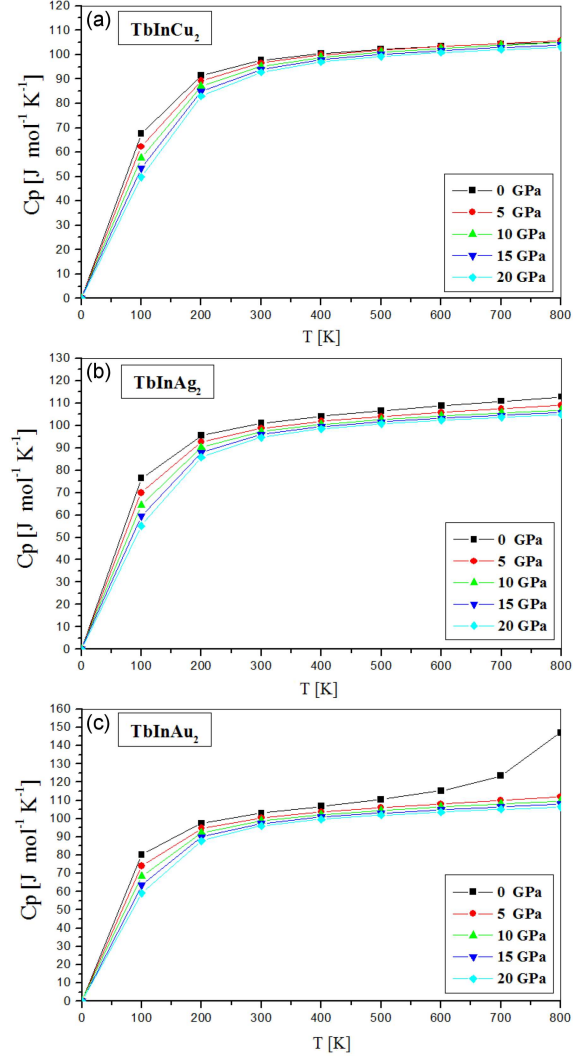


Fig. 13. (a, b, c) The variation of heat capacity C_p as a function of temperature for TbInZ_2 ($Z = \text{Cu}, \text{Ag}, \text{Au}$) at different pressures.

temperature. Entropy can be interpreted as a measure of the degree of disorder in a system at the microscopic level. The higher the entropy of the system, the less its elements are ordered, linked to each other, capable of producing mechanical effects.

4. Conclusion

We studied the structural, electronic, magnetic and thermal properties of the three compounds TbInZ_2 ($Z = \text{Cu}, \text{Ag}$ and Au), using an *ab initio* method, i.e., full-potential linearized augmented plane wave (FP-LAPW) method implemented in Wien2k code and within the framework of the density functional theory. The exchange and correlation potential has been treated as part of the generalized gradient approximation (GGA-PBE).

First, the structural properties at equilibrium have been determined, such as the lattice parameter, total energies and the bulk modulus and its

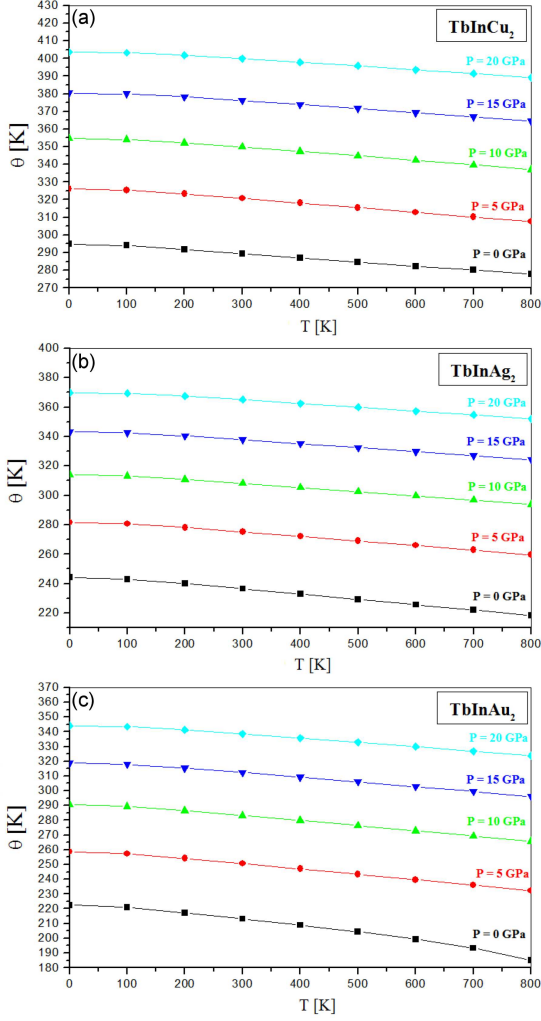


Fig. 14. (a, b, c) The variation of debye temperature as a function of temperature for TbInZ_2 (Z = Cu, Ag, Au) at different pressures.

derivative. The results obtained for the three compounds fit the experimentally determined values very well, which leads to the conclusion that TbInZ_2 (Z = Cu, Ag, Au) alloys are stable in the ferromagnetic state (FM). Band structures of the TbInZ_2 (Z = Cu, Ag, Au) compounds have been calculated. We notice the metallic and paramagnetic character for the investigated materials, therefore they are considered as very good candidates for spintronic applications. Both total and local magnetic moments of TbInZ_2 (Z = Cu, Ag, Au) alloys are presented — they are mainly characterized by the high contribution of the Tb- f atom. The thermodynamic properties of TbInZ_2 (Z = Cu, Ag, Au) compounds have been studied via the Debye quasi-harmonic model. The results obtained clearly indicated that the temperature increases the structural parameters, while the pressure decreases them, showing their opposite effects. However, we conclude that thermodynamic quantities such as heat capacity and system disorder increase with increasing tem-

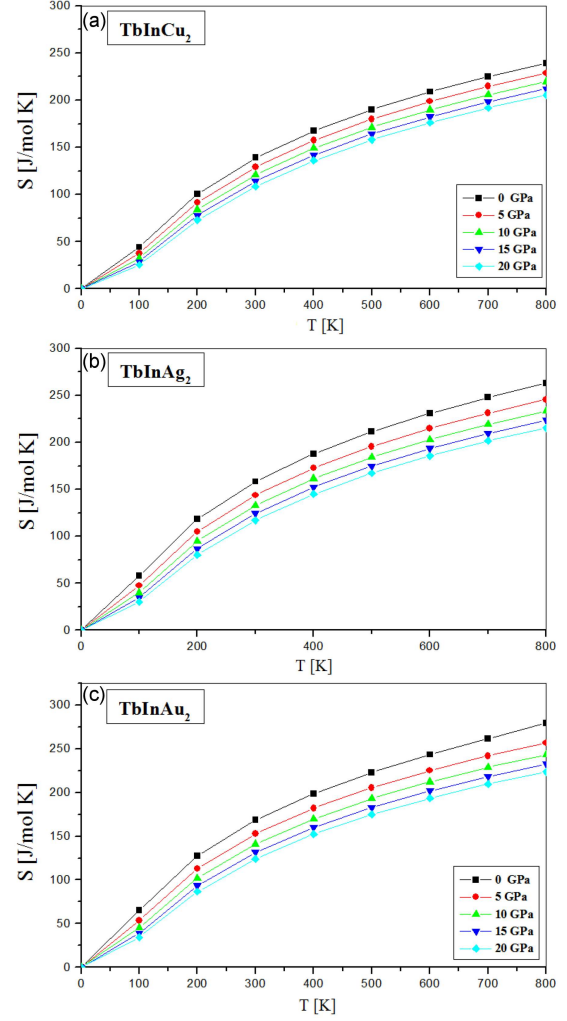


Fig. 15. (a, b, c) The variation of entropy as a function of temperature for TbInZ_2 (Z = Cu, Ag, Au): at different pressures.

perature and decrease with increasing pressure, and it is clear that the three materials have high Debye temperatures. In the absence of theoretical and experimental results concerning these parameters, our study consists of a detailed predictive study.

References

- [1] A. Hirohata, K. Yamada, Y. Nakatani, I.-L. Prejbeanu, B. Diény, P. Pirro, B. Hillebrands, *J. Magn. Magn. Mater.* **509**, 166711 (2020).
- [2] R.M. Galera, J. Pierre, E. Siaud, A.P. Murani, *J. Less Common Met.* **97**, 151 (1984).
- [3] I. Felner, *Solid State Commun.* **56**, 315 (1985).
- [4] M.J. Besnus, J.P. Kappler, M.F. Ravet, A. Meyer, R. Lahiouel, J. Pierre, E. Siaud, G. Nieva, J. Sereni, *J. Less Common Met.* **120**, 101 (1986).

- [5] Yang Zhou, JianMin Zhang, *Appl. Phys. A* **125**, 800 (2019).
- [6] P. Blaha, K. Schwarz, G.K. Madsen et al., "Wien2k: An Augmented Plane Wave + Local Orbitals Program for Calculating Crystal Properties", Technische Universität Wien, Wien 2001.
- [7] Y. Mokrousov, G. Bihlmayer, S. Blügel, *Phys. Rev. B* **72**, 045402 (2005).
- [8] A. Touia, C. Khobzaoui, M. Benkhaled, M. Fodil, *J. Supercond. Nov. Magn.* **34**, 1865 (2021).
- [9] A.Touia, K. Benyahia, A. Tekin, *J. Supercond. Nov. Magn.* **34**, 2689 (2021).
- [10] J.P. Perdew, J.A.Chevary, S.H. Vosko, K.A. Jackson, M.R. Pederson, D.J. Singh, C. Fiolhais, *Phys. Rev. B* **48**, 4978 (1993).
- [11] J. Perdew, K. Burke, M. Ernzerhof, Perdew, Burke, Ernzerhof Reply. *Phys. Rev. Lett.* **80**, 891 (1998).
- [12] V. Sokolovskiy, M. Zagrebin, V.D. Buchelnikov, *J. Magn. Magn. Mater.* **476**, 546 (2019).
- [13] F.D. Murnaghan, *PNAS* **30**, 244 (1944).
- [14] A. Touia, M. Ameri, I. Ameri, *Optik*. **126**, 3253 (2015).
- [15] I. Yahiaoui, A. Lazreg, Z.Dridi, Y. Al-Douri, B.Bouhafs, *J. Supercond. Nov. Magn.* **30**, 421 (2017).
- [16] S.A. Khandy, I. Islam, A.Laref, M. Gogolin, A.K. Hafiz, A.M. Siddiqui, *Int. J. Energy Res.* **44**, 2594 (2020).
- [17] A. Touia, M. Benkhaled, C. Khobzaoui, M. Fodil, *J. Supercond. Nov. Magn.* **34**, 2865 (2021).
- [18] M. Blanco, E. Francisco, V. Luana, *Comput. Phys. Commun.* **158**, 57 (2004).
- [19] S.M. Laoufi, A. Touia, M. Ameri, I. Ameri, F. Boufadi, K. Boudia, A. Slamani, F. Belkharroubi, Y. Al-Douri, *Optik* **127**, 7382 (2016).
- [20] E. Francisco, J. Recio, M. Blanco, A.M. Pendás, A. Costales, *J. Phys. Chem. A* **102**, 1595 (1998).
- [21] F. Khelfaoui, M. Ameri, D. Bensaid, I. Ameri, Y. Al-Douri, *J. Supercond. Nov. Magn.* **31**, 3183 (2018).
- [22] G.K.H. Madsen, D.J. Singh, *Comput. Phys. Commun.* **175**, 67 (2006).